

Bulk ferromagnetic tips for spin-polarized scanning tunneling microscopy

メタデータ	言語: eng 出版者: 公開日: 2019-04-19 キーワード (Ja): キーワード (En): 作成者: メールアドレス: 所属:
URL	https://doi.org/10.24517/00053905




This work is licensed under a Creative Commons Attribution-NonCommercial-ShareAlike 3.0 International License.



Bulk ferromagnetic tips for spin-polarized scanning tunneling microscopy

Cite as: Rev. Sci. Instrum. **90**, 013704 (2019); <https://doi.org/10.1063/1.5063759>

Submitted: 01 October 2018 . Accepted: 08 January 2019 . Published Online: 25 January 2019

Masahiro Haze , Hung-Hsiang Yang, Kanta Asakawa, Nobuyuki Watanabe, Ryosuke Yamamoto, Yasuo Yoshida , and Yukio Hasegawa 



View Online



Export Citation



CrossMark



Bulk ferromagnetic tips for spin-polarized scanning tunneling microscopy

Cite as: Rev. Sci. Instrum. 90, 013704 (2019); doi: 10.1063/1.5063759

Submitted: 1 October 2018 • Accepted: 8 January 2019 •

Published Online: 25 January 2019



Masahiro Haze,^{1,2,a)}  Hung-Hsiang Yang,¹ Kanta Asakawa,¹ Nobuyuki Watanabe,¹ Ryosuke Yamamoto,^{1,b)} Yasuo Yoshida,^{1,3,c)}  and Yukio Hasegawa¹ 

AFFILIATIONS

¹Institute for Solid State Physics, The University of Tokyo, Kashiwa, Chiba 277-8581, Japan

²Department of Physics, Kyoto University, Sakyo-ku, Kyoto 606-8502, Japan

³Department of Physics, Kanazawa University, Kanazawa, Ishikawa 920-1192, Japan

^{a)}haze.masahiro.2x@kyoto-u.jp

^{b)}Present address: Department of Chemistry, The University of Tokyo, Tokyo, Japan.

^{c)}Author to whom correspondence should be addressed: yyoshida@se.kanazawa-u.ac.jp

ABSTRACT

We characterized the performance of electrochemically etched bulk Fe and Ni tips as a probe of spin-polarized scanning tunneling microscopy (SP-STM). Through the observation of the striped contrast on the conical spin-spiral structure formed in Mn double layers on a W(110) substrate, the capability of both the tips to detect the magnetic signal was clarified. We also confirmed that the magnetized direction of the Fe and Ni tips can be flipped between the two out-of-plane directions by external magnetic fields. Our results demonstrate that the *ex-situ* prepared tips are reliable in SP-STM for the samples that are not susceptible to a stray magnetic field.

Published under license by AIP Publishing. <https://doi.org/10.1063/1.5063759>

I. INTRODUCTION

Spin-polarized scanning tunneling microscopy (SP-STM) is one of the most advanced scanning probe techniques suitable for the research of condensed matter physics.^{1,2} SP-STM allows us to study atomic-scale magnetism in real space, and its application to strongly correlated electron materials³⁻⁵ and spintronics devices are highly expected. Fabricating reliable spin-polarized tips is, however, not an easy task. In a conventional method, a spin-polarized tip is made by depositing ferromagnetic (e.g., Fe,^{6,7} Gd⁸) or antiferromagnetic (e.g., Cr,⁹ Mn¹⁰) materials onto a tip apex of a nonmagnetic W tip. Although such tips provided a lot of reliable SP-STM results,² there are some disadvantages. First, they require complicated *in-situ* preparation procedures under ultra-high-vacuum (UHV) conditions. Second, a tip may become dull due to the deposited materials. Third, the deposited magnetic materials at their apices are easily lost through accidental tip crash or bias voltage pulses for *in-situ* tip treatment.

To lower the hurdles, tips made of bulk magnetic materials that are sharpened by electrochemical etching have been utilized in recent years. These tips never lose their spin-polarization in principle. Because of its negligible stray field, an antiferromagnetic Cr tip is widely used.¹¹⁻¹⁹ However, the drawback of the tip is its insensitivity to an external magnetic field. Unless ferromagnetic materials are picked up on the apex,^{15,16} the tip magnetization direction is not controllable because of no net magnetic moment and the strong antiferromagnetic exchange coupling. On the other hand, when the magnetism of a target sample is robust against an external magnetic field, such as antiferromagnetic materials with strong exchange interactions, ferromagnetic bulk tips are still good choices since the magnetizations can be controlled by magnetic fields.

As ferromagnetic materials, there are a lot of choices, such as single metals and alloys. While ferromagnetic tips made from alloys are also candidates for spin-polarized tips,^{20,21} we here focus on single metals because they are commercially available and easy to handle. In addition, we

focus on soft ferromagnetic materials in terms of the controllability of the magnetizations. The typical and abundant elemental soft ferromagnetic material is Fe. Ni is also conventional and has the advantage that it does not easily oxidize in the air at room temperature. Furthermore, Ni has smaller magnetic moments ($0.6 \mu_B$) than Fe ($2.2 \mu_B$), which produces a smaller stray field. This smaller stray field is also advantageous as an SP-STM tip because its influence to magnetic structures of target samples is reduced. Although both tips have been used for STM measurements,²²⁻²⁵ convincing SP-STM results with these tips are still lacking.

When we observe contrasts in SP-STM, it is not easy to judge whether they arise from the magnetic origin or not. The most reliable way to confirm the magnetic origin is through the observation of contrast reversal due to the switching of the magnetization direction of the tip or sample when an external magnetic field is flipped. Here, we focus on these two ferromagnetic materials; we report the performances of bulk Fe and Ni tips in SP-STM in external magnetic fields and compare them with those of a bulk Cr tip, which is already known as a reliable SP-STM tip.

In order to characterize the spin-polarized tips, a well-investigated and reliable reference sample is needed. In this study, we selected Mn double layers (DLs) on a W(110) substrate, whose magnetic structure has been well-investigated by SP-STM.²⁶⁻²⁹ Its strong signal and non-collinear magnetic structure are useful to characterize SP-STM tips. As will be demonstrated below, we clearly observed the magnetic contrast of Mn DLs with both Fe and Ni tips, indicating that both tips are reliable enough as SP-STM tips for the samples which are robust against a stray magnetic field. We also found that the magnetization direction of the tips is controllable with an external magnetic field along out-of-plane directions.

II. PREPARATION OF TIPS

We formed a bulk Cr tip from a Cr rod with a square cross section cut from a 99.99% Cr plate using a diamond cutter. For bulk Fe and Ni tips, 99.995% Fe and 99.995% Ni wires were used. The diameters of both Fe and Ni wires are 0.4 mm. The Fe and Ni tips were formed by electrochemical etching in a 2M HCl electrolyte. For a Cr tip, we used a 2M KOH as an etching solution. Figure 1 shows a schematic of the setup of electrochemical etching. A Cr, Ni, or Fe rod/wire was connected to a power supply and dipped into the solution as an anode, and for a cathode, we used a W wire. The area of the anode that is dipped in the electrolyte is covered by a polyvinyl chloride (PVC) tube to avoid etching the wires, except around the surface of the solution. When the rod/wire is cut electrochemically, we can obtain two very sharp tips; the upper side without a PVC tube and the lower side covered by the tube. Both tips can be used as an SP-STM tip, but the lower side tip is often sharper than the upper one. For the etching, we used AC or DC power supply depending on the situation. To make sharper tips, it is better to proceed the etching as slowly as possible by using a DC power supply. However, since the etching rate with a DC voltage is rather low and thus it takes too much time, we first etch a tip by using an AC power

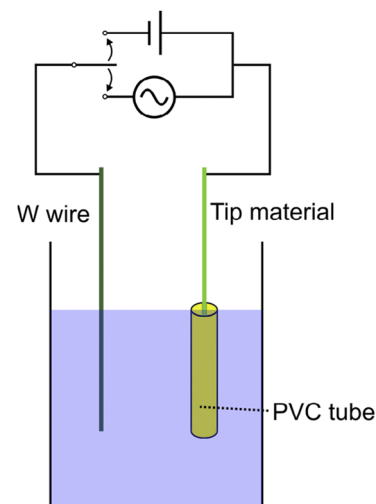


FIG. 1. Schematic of the setup of the electrochemically etching.

supply with $V_{AC} = 2$ V until just before the cutting of the rod/wire. After cutting the rod/wire with a DC voltage with $V_{DC} = 15$ V to form very sharp tips, we dip the tips into hot water to remove the solution. After cutting the tip to 8 mm, we set it with 2 mm sticking out from a tip holder. We put the tip on the STM head without any *in-situ* treatment. We treat the tips by applying voltage pulses up to 10 V between the tip and surface and/or dipping into the surface.

Typical scanning electron microscopy (SEM) images of bulk Fe and Ni tips are displayed in Fig. 2. The estimated radii of the tip apices are less than 100 nm. Prior to SP-STM measurements, we performed STM and tunneling spectroscopy measurements on the Au(111) surface with these tips, and the obtained results are consistent with previous studies with a nonmagnetic tip, suggesting high performance of the bulk magnetic tips as a standard STM probe. To prevent the tips from oxidation, we keep them in the vacuum desiccator after etching. But even in a desiccator, Fe and Cr tips gradually deteriorate if we keep them too long, like several years. Ni tips normally do not change.

III. STM SETUP AND SAMPLE

The experiments have been performed with a low-temperature UHV STM (Unisoku USM-1300S with an RHK R9 controller), in which the tip and sample are cooled down to 5 K. Superconducting magnets are equipped to apply magnetic fields perpendicular and parallel to the sample surface up to ± 2 T and ± 1 T, respectively. All STM and SP-STM measurements are performed with the constant current mode at 5 K.

A W(110) substrate was prepared by several cycles of flashing above 2300 K in UHV and annealing at 1500 K in an oxygen atmosphere of 1×10^{-4} Pa. We deposited Mn onto the substrate for 70 s at a deposition rate of 1.5 ml/min from a Ta crucible heated by electron bombardment. In order to achieve step-flow growth, Mn deposition was performed just after the flashing to ensure the high mobility of the deposited atoms.³⁰

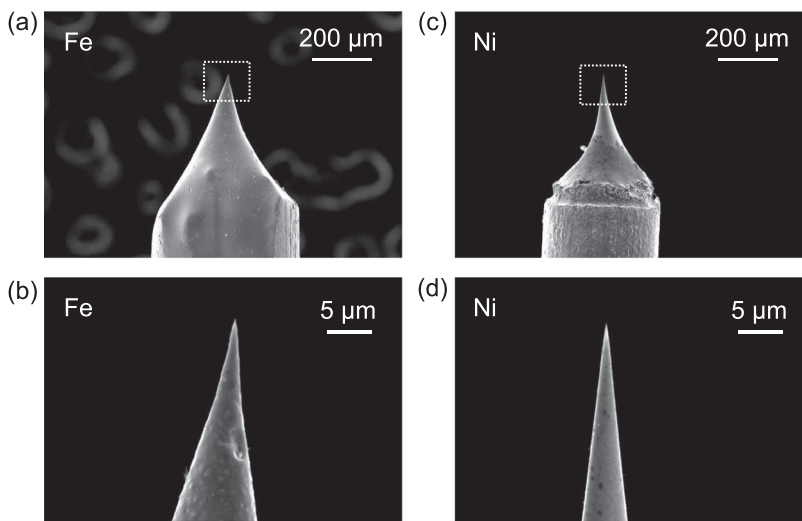


FIG. 2. [(a) and (b)] SEM images of a bulk Fe tip with low (×100) and high (×3000) magnifications. [(c) and (d)] SEM images of a bulk Ni tip with low (×100) and high (×3000) magnifications.

IV. SP-STM MEASUREMENTS

In order to confirm the spin spiral structure of Mn DL and its insensitivity to the magnetic fields, we perform SP-STM measurements using a bulk Cr tip. Figures 3(a) and 3(b) show the topographic STM and simultaneously obtained dI/dV images on the Mn thin films taken with a bulk Cr tip,

respectively. On the surface, a spin-polarized contrast appears in a dI/dV image taken at around the sample bias voltage $V_S = 0$,²⁸ and the images shown in Fig. 3 were taken at -40 mV. ML and DL shown in Fig. 3(a) indicate the regions of monolayers and double layers, respectively. In the DL region, a striped pattern along the [001] direction whose periodicity is about 2.0 nm is clearly resolved in the dI/dV image. The magnetic

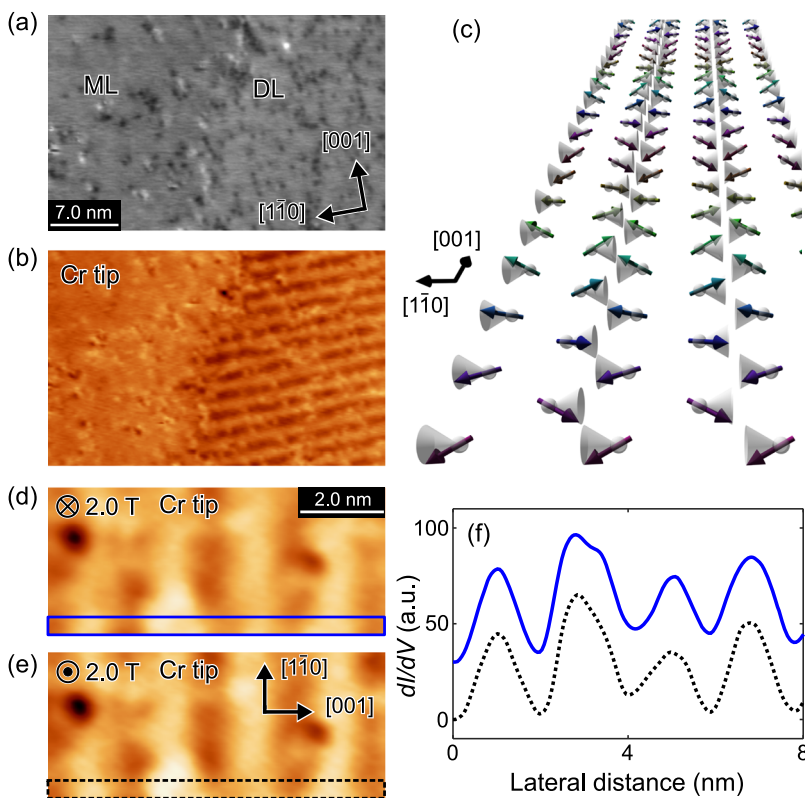


FIG. 3. [(a) and (b)] A topographic STM image of Mn/W(110) with a bulk Cr tip and a simultaneously recorded dI/dV image. Tunneling current $I_T = -1$ nA, sample bias voltage $V_S = -40$ mV, bias-modulation frequency $f_{mod} = 1.877$ kHz, and bias-modulation amplitude $V_{mod} = 30$ mV. (c) Schematic spin structures of conical-spin-spiral rotation of Mn DL propagating along the [001] direction. [(d) and (e)] Spin-resolved dI/dV images taken on the same area in the out-of-plane magnetic fields of $B = +2.0$ T and $B = -2.0$ T, respectively. Both images are taken with the same bulk Cr tip. (f) The blue solid and black dotted lines indicate the line profiles taken in the boxed blocks in (d) and (e), respectively.

contrast in SP-STM varies as the cosine of the relative angle θ between the tip and sample magnetization directions. Therefore, the bright- and dark-contrasted regions are Mn rows that have magnetization components parallel and antiparallel to the tip magnetization direction. In the ML region, no periodic pattern is observed, despite the presence of a different type of spin spiral structure.³¹ This is due to different conditions of magnetic contrast for ML: the magnetic contrast of ML can be found in a topographic image of +10 mV, but not in a dI/dV image of -40 mV.²⁸

From this result, we can confirm the conical spin-spiral structure which propagates along the [001] direction in the DL region, as shown in the schematic of Fig. 3(c).²⁶ It has been reported that the magnetization direction of a bulk Cr tip is arbitrary and differs from one tip to another.¹⁴ This is probably because the tip apex domain of bulk Cr tips does not have preferential orientation. In our measurement, the fine structure along the [110] direction due to the in-plane antiferromagnetic components^{26,29} is not resolved (Fig. 3), which means that the magnetization direction of our Cr bulk tip is mostly out-of-plane and the tip does not have the in-plane sensitivity.

Figures 3(d) and 3(e) show the spin-polarized dI/dV images taken on the same DL area in the perpendicular magnetic fields of $B = \pm 2$ T. The striped pattern is clearly resolved in both images, and there is essentially no change in the contrast between the two images. The line profiles [Fig. 3(f)] taken in the boxed blocks in Figs. 3(d) and 3(e) match well with each other, which also means no phase shift in the sinusoidal waves.

It has been reported that magnetization of a Cr tip is not reversed by an external magnetic field at least up to $B = 4$ T,¹⁴ unless ferromagnetic materials are adsorbed on the tip apex.¹³⁻¹⁵ In the present case, we do not have any ferromagnetic materials on the surface, and thus, the chance for reversal of the Cr tip magnetization is low. Therefore, the same contrast between the above two images indicates that the spin spiral structure of Mn DL is also not influenced by the magnetic fields, showing that this sample is suitable for investigating the field dependence of tip magnetizations.

Figures 4(a) and 4(b) show the topographic and simultaneously taken dI/dV images with a bulk Fe tip on Mn DL on W(110). The striped pattern due to the spin-spiral structure is resolved in Fig. 4(b), and more clearly in a zoomed image [Fig. 4(c)] and its line profile. We performed a similar measurement using a bulk Ni tip, as shown in Figs. 4(d)–4(f), and confirmed the striped pattern. These results clearly demonstrate that both bulk Fe and Ni tips work well as an SP-STM tip. All the measurements for Fig. 4 were done in the perpendicular magnetic field, and all SP-STM images show only the spin-spiral contrast along the [001] directions. This indicates that the tip magnetization is fully polarized along the out-of-plane direction by the external magnetic field.

To check the response of the tips to magnetic fields, we performed SP-STM measurements at $B = \pm 2.0$ T. Figures 5(a)–5(c) show the topographic and corresponding dI/dV images taken with a bulk Fe tip at $B = +2.0$ T and $B = -2.0$ T, respectively. Note that around 10 nm lateral offset was needed for taking both images in the same field of view,

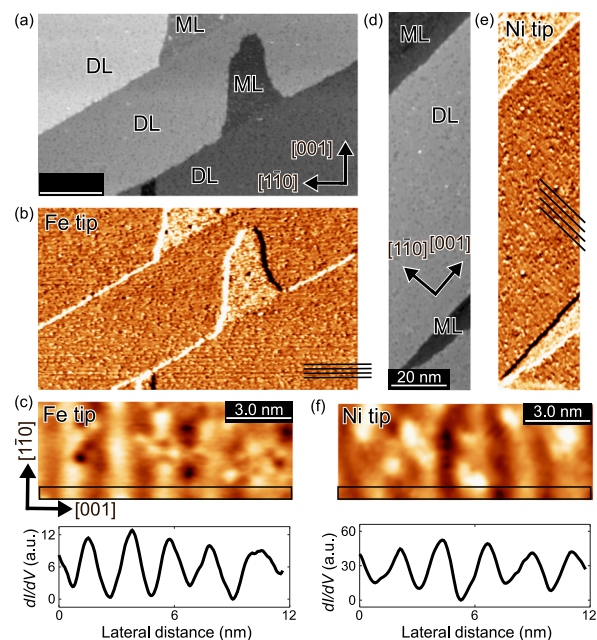


FIG. 4. [(a) and (b)] Topographic and corresponding dI/dV images taken with a bulk Fe tip, respectively ($I_T = -0.3$ nA, $V_S = -100$ mV, $f_{mod} = 1.877$ kHz, $V_{mod} = 35$ mV, and $B = 1.0$ T). (c) The zoomed-in view of a dI/dV image into a DL region and a cross section taken in the boxed area ($I_T = -1$ nA, $V_S = -50$ mV, $f_{mod} = 1.877$ kHz, $V_{mod} = 20$ mV, and $B = 1$ T). [(d) and (e)] Topographic and corresponding dI/dV images taken with a bulk Ni tip, respectively ($I_T = -1$ nA, $V_S = -100$ mV, $f_{mod} = 1.877$ kHz, $V_{mod} = 30$ mV, and $B = 0.5$ T). (f) The zoomed-in view of a dI/dV image into a DL region and a cross section taken in the boxed area ($I_T = -1$ nA, $V_S = -50$ mV, $f_{mod} = 1.877$ kHz, and $V_{mod} = 20$ mV). The black lines in (b) and (e) are a guide for finding the stripe pattern due to the spin spiral.

which is likely due to the deformation of a ferromagnetic tip by magnetic fields. In the dI/dV images of Figs. 5(b) and 5(c), the 180° phase shift of the sinusoidal patterns is observed. Figure 5(d) displays the line sections taken along the boxed areas in the dI/dV images of Figs. 5(b) and 5(c). Both of them show the sinusoidal patterns, but the phases are shifted by about 180° . Since the magnetic structure of Mn DL is not affected by external magnetic fields up to 2.0 T, as mentioned before, this result indicates that the magnetized direction of a bulk Fe tip is inverted by the external magnetic field.

Figures 5(e)–5(g) show the topographic and dI/dV images taken with a bulk Ni tip in $B = +2.0$ T and $B = -2.0$ T, respectively, and Fig. 5(h) shows the line sections taken along the boxed area in Figs. 5(f) and 5(g). We here note that we experienced ~ 5 nm lateral offset between the images of Figs. 5(f) and 5(g) again due to the same reason mentioned above. This set of images basically provides the same information shown above with that taken with a bulk Fe tip, demonstrating that the magnetized direction of both Fe and Ni tips can be controlled by external magnetic fields. We also attempted SP-STM measurements with those tips in in-plane magnetic fields up to 1 T and observed spin-polarized contrasts. However, we could not find the same area observed before applying the fields, probably due to too much bending of the tip by the fields,

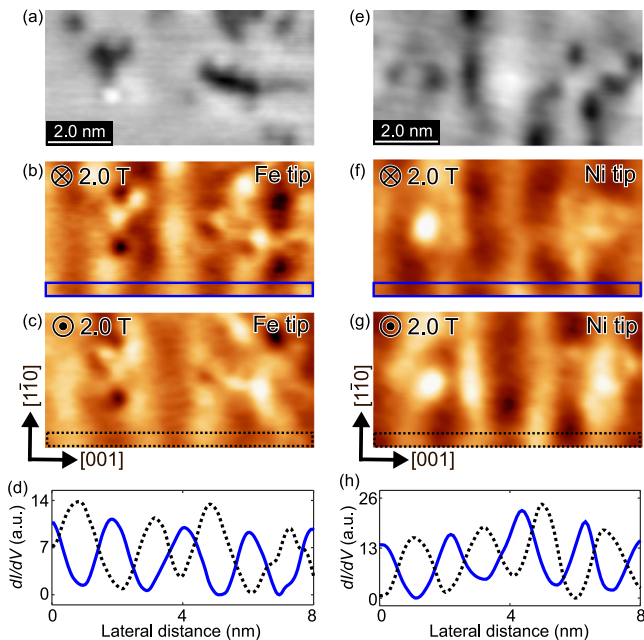


FIG. 5. (a) A topographic image taken with a bulk Fe tip. [(b) and (c)] Simultaneously obtained spin-polarized dI/dV images in $B = +2.0$ T for (b) and $B = -2.0$ T for (c) ($I_T = -1$ nA, $V_S = -50$ mV, $f_{mod} = 1.877$ kHz, and $V_{mod} = 20$ mV). (d) The blue solid and black dotted lines indicate the line sections taken along the boxed area in (b) and (c), respectively. (e) A topographic image taken with a bulk Ni tip. [(f) and (g)] Simultaneously obtained spin-polarized dI/dV images in $B = +2.0$ T for (f) and $B = -2.0$ T for (g) ($I_T = 1$ nA, $V_S = 50$ mV, $f_{mod} = 0.971$ kHz, and $V_{mod} = 10$ mV). (h) The blue solid and black dotted lines indicate the line sections taken along the boxed areas in (f) and (g), respectively.

and therefore, we could not characterize the in-plane-field dependence of tip magnetizations. In addition, we noticed that deformation of the tip due to the out-of-plane magnetic fields causes tip crashes, unless we retracted the tip far enough.

V. COMPARISON WITH OTHER TIPS

Here, we compare bulk ferromagnetic Fe and Ni tips with other magnetic tips. As demonstrated above, bulk ferromagnetic Ni and Fe tips work well as spin-polarized tips and the magnetization directions can be controlled easily. Although Fe-coated W tips also fulfill these conditions, there are three disadvantages. First, it is difficult to make tips. Second, magnetization may be lost by accidental tip crashes or applied bias voltage pulses. Third, since the shape of the tip apex is not well organized, it is likely to be a multiple tip.

Bulk antiferromagnetic Cr tips do not have these disadvantages, but it is difficult to control the magnetization directions of the tips by external magnetic fields. Moreover, the magnetization direction is not well defined. Other research groups characterized the tip differently (tilted,¹² in-plane¹³) at a zero magnetic field. This is probably due to the difference in material quality. Purities of commercially available Cr materials are relatively low compared to those of other 3d transition magnets. Since it is known that the magnetic properties

of Cr are affected by the types of impurities,³² tip magnetization directions could be affected depending on the types of impurities included.

The difference in the magnetization direction probably also comes from orientations of tip apices. As we mentioned before, Cr tips are usually made from Cr rods which are cut from polycrystalline Cr plates. Thus the orientation of tip apices differs from one another, which affects tip magnetization directions.

One and rather critical disadvantage of bulk Fe ferromagnetic tips is its large stray magnetic field. Therefore, this tip is more suitable for SP-STM measurements on samples whose magnetism is robust against external magnetic fields such as antiferromagnetic materials with strong spin interactions. The stray magnetic field of Ni is much weaker than Fe because the magnetization is about 3.5 times smaller than Fe. This could make Ni tips more versatile than Fe tips.

VI. CONCLUSION

We characterized the properties of bulk Fe and Ni tips in SP-STM measurements on Mn DL grown on W(110), which is a prototypical SP-STM sample. We revealed that both bulk Fe and Ni tips work well as SP-STM tips for the samples that are insensitive to a stray magnetic field and their tip magnetization directions can be controlled in the out-of-plane directions by external magnetic fields. This work provides an easy way to prepare SP-STM tips, which may contribute to the promotion of nano-scale studies on strongly correlated electron materials and spintronics devices by using the SP-STM technique.

ACKNOWLEDGMENTS

We thank Masayuki Hamada for his technical assistance in SEM measurements. This work was partially supported by JSPS KAKENHI Grant Nos. JP25707025, JP26110507, JP26120508, JP16K17744, JP16H01534, and JP18H04480.

REFERENCES

- M. Johnson and J. Clarke, *J. Appl. Phys.* **67**, 6141 (1990).
- R. Wiesendanger, *Rev. Mod. Phys.* **81**, 1495 (2009).
- M. Enayat, Z. Sun, U. R. Singh, R. Aluru, S. Schmaus, A. Yaresko, Y. Liu, C. Lin, V. Tsurkan, A. Loidl, J. Deisenhofer, and P. Wahl, *Science* **345**, 653 (2014).
- S. Manna, A. Kamlapure, L. Cornils, T. Hänke, E. Hedegaard, M. Bremholm, B. Iversen, P. Hofmann, J. Wiebe, and R. Wiesendanger, *Nat. Commun.* **8**, 14074 (2017).
- S. Choi, H. J. Choi, J. M. Ok, Y. Lee, W.-J. Jang, A. T. Lee, Y. Kuk, S. Lee, A. J. Heinrich, S.-W. Cheong, Y. Bang, S. Johnston, J. S. Kim, and J. Lee, *Phys. Rev. Lett.* **119**, 227001 (2017).
- M. Bode, M. Getzlaff, and R. Wiesendanger, *Phys. Rev. Lett.* **81**, 4256 (1998).
- A. Kubetzka, P. Ferriani, M. Bode, S. Heinze, G. Bihlmayer, K. Von Bergmann, O. Pietzsch, S. Blügel, and R. Wiesendanger, *Phys. Rev. Lett.* **94**, 087204 (2005).
- O. Pietzsch, A. Kubetzka, M. Bode, and R. Wiesendanger, *Phys. Rev. Lett.* **84**, 5212 (2000).

- ⁹A. Kubetzka, M. Bode, O. Pietzsch, and R. Wiesendanger, *Phys. Rev. Lett.* **88**, 057201 (2002).
- ¹⁰H. Yang, A. R. Smith, M. Prikhodko, and W. R. Lambrecht, *Phys. Rev. Lett.* **89**, 226101 (2002).
- ¹¹A. Li Bassi, C. Casari, D. Cattaneo, F. Donati, S. Foglio, M. Passoni, C. Bottani, P. Biagioni, A. Brambilla, M. Finazzi, F. Ciccacci, and L. Duò, *Appl. Phys. Lett.* **91**, 173120 (2007).
- ¹²A. Schlenhoff, S. Krause, G. Herzog, and R. Wiesendanger, *Appl. Phys. Lett.* **97**, 083104 (2010).
- ¹³M. Corbetta, S. Ouazi, J. Borme, Y. Nahas, F. Donati, H. Oka, S. Wedekind, D. Sander, and J. Kirschner, *Jpn. J. Appl. Phys.* **51**, 030208 (2012).
- ¹⁴N. Romming, C. Hanneken, M. Menzel, J. E. Bickel, B. Wolter, K. von Bergmann, A. Kubetzka, and R. Wiesendanger, *Science* **341**, 636 (2013).
- ¹⁵K. Doi, E. Minamitani, S. Yamamoto, R. Arafune, Y. Yoshida, S. Watanabe, and Y. Hasegawa, *Phys. Rev. B* **92**, 064421 (2015).
- ¹⁶S. Nadj-Perge, I. K. Drozdov, J. Li, H. Chen, S. Jeon, J. Seo, A. H. MacDonald, B. A. Bernevig, and A. Yazdani, *Science* **346**, 602 (2014).
- ¹⁷A. Sonntag, J. Hermenau, A. Schlenhoff, J. Friedlein, S. Krause, and R. Wiesendanger, *Phys. Rev. Lett.* **112**, 017204 (2014).
- ¹⁸A. Sonntag, J. Hermenau, S. Krause, and R. Wiesendanger, *Phys. Rev. Lett.* **113**, 077202 (2014).
- ¹⁹S. Krause, A. Sonntag, J. Hermenau, J. Friedlein, and R. Wiesendanger, *Phys. Rev. B* **93**, 064407 (2016).
- ²⁰W. Wulfhekel and J. Kirschner, *Appl. Phys. Lett.* **75**, 1944 (1999).
- ²¹H. Ding, W. Wulfhekel, and J. Kirschner, *Europhys. Lett.* **57**, 100 (2002).
- ²²S. F. Alvarado and P. Renaud, *Phys. Rev. Lett.* **68**, 1387 (1992).
- ²³R. Wiesendanger, I. Shvets, and J. Coey, *J. Vac. Sci. Technol., B: Microelectron. Nanometer Struct.–Process., Meas., Phenom.* **12**, 2118 (1994).
- ²⁴M. Cavallini and F. Biscarini, *Rev. Sci. Instrum.* **71**, 4457 (2000).
- ²⁵H. Chen, W. Xiao, X. Wu, K. Yang, and H.-J. Gao, *J. Vac. Sci. Technol., B: Nanotechnol. Microelectron.: Mater., Process., Meas., Phenom.* **32**, 061801 (2014).
- ²⁶Y. Yoshida, S. Schröder, P. Ferriani, D. Serrate, A. Kubetzka, K. von Bergmann, S. Heinze, and R. Wiesendanger, *Phys. Rev. Lett.* **108**, 087205 (2012).
- ²⁷K. von Bergmann, M. Menzel, D. Serrate, Y. Yoshida, S. Schröder, P. Ferriani, A. Kubetzka, R. Wiesendanger, and S. Heinze, *Phys. Rev. B* **86**, 134422 (2012).
- ²⁸M. Haze, Y. Yoshida, and Y. Hasegawa, *Phys. Rev. B* **95**, 060415(R) (2017).
- ²⁹M. Haze, Y. Yoshida, and Y. Hasegawa, *Sci. Rep.* **7**, 13269 (2017).
- ³⁰M. Bode, S. Heinze, A. Kubetzka, O. Pietzsch, M. Hennefarth, M. Getzlaff, R. Wiesendanger, X. Nie, G. Bihlmayer, and S. Blügel, *Phys. Rev. B* **66**, 014425 (2002).
- ³¹M. Bode, M. Heide, K. Von Bergmann, P. Ferriani, S. Heinze, G. Bihlmayer, A. Kubetzka, O. Pietzsch, S. Blügel, and R. Wiesendanger, *Nature* **447**, 190 (2007).
- ³²R. S. Fishman and S. H. Liu, *Phys. Rev. B* **45**, 12306 (1992).